Available online at www.sciencedirect.com

ScienceDirect

Energy Procedia 53 (2014) 34 – 43

Energy Procedia

EERA DeepWind'2014, 11th Deep Sea Offshore Wind R&D Conference

Multiphysics 3D modelling of ironless permanent magnet generators

Z. Zhang[a], S. M. Muyeen[b], A. Al-Durra[b], R. Nilssen[a], A. Nysveen[a]

[a]*Norwegian University of Science and Technology, 7491, Trondheim, Norway*
[b]*The Petroleum Institute, P. O. Box 2533, Abu Dhabi, United Arab Emirates*

Abstract

Analytical method is widely used for the preliminary design and optimization of electrical machines. It has short calculation time and low computational cost (cost of simulation codes and supporting hardware), but the calculate result is normally considered to be not as accurate as finite element method (FEM). On the other hand, it is time-consuming to optimize machines with FEM if the optimization is not parallelized. Parallelizing optimization requires many licenses when commercial FEM codes are used, which can be very expensive. Ironless permanent magnet generator has large diameter and small aspect ratio, therefore, multiphysics approach is expected to be used for investigating the magnetic and thermal field. To address the above challenges, this paper presents a multiphysics modelling strategy for the design and optimization of ironless permanent magnet generators. Open-source codes are used to reduce the computational cost. A design example is presented to demonstrate the detail of this design method. This approach is expected to be used in super computer in the future, so that the calculation time can be largely reduced.

Selection and peer-review under responsibility of SINTEF Energi AS
Keywords: Finite element method; ironless permanent magnet generators; machine optimization; multipysics modelling.

1. Introduction

Large-scale computing resources (LCR), e.g. clusters, super computers, are used to handle computation-demanding problems, such as the models for fluid dynamics and structural mechanics. This is due to the significant speedup ratio achieved with high performance computing techniques. However, it is not common to design electrical machines with LCR.

There are two main reasons. First, machine designers normally prefer to design and optimize machines with analytical approach, and finite element analysis (FEA) is conducted later to verify the optimization result. Such a design process can be executed with ordinary PCs, desktops or workstations. However, the prerequisite for making this design procedure feasible is the good accuracy of the analytical method used. Machine designers therefore have to put a lot of efforts for developing suitable analytical methods in terms of high accuracy and short calculation time. Unfortunately, depending on the specific analytical method used, significant errors may be produced [1]. Consequently,

* Zhaoqiang Zhang. Tel.: +0047-73594271.
E-mail address: zhaoqiang.zhang@ntnu.no

Selection and peer-review under responsibility of SINTEF Energi AS
doi:10.1016/j.egypro.2014.07.213

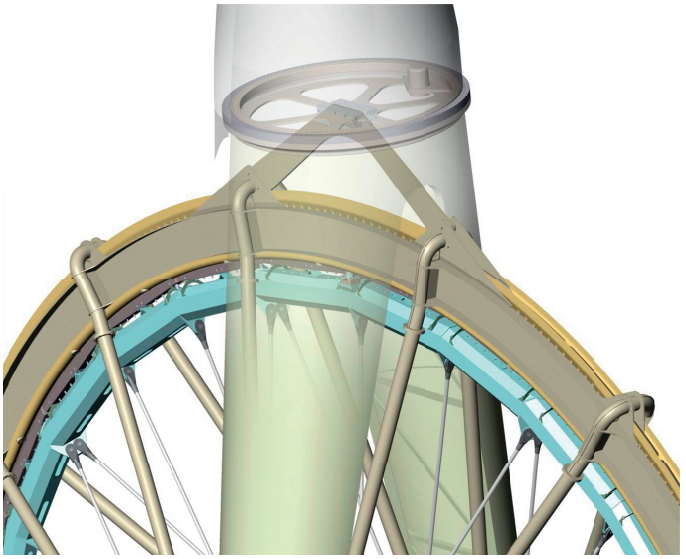

Fig. 1. The concept of integration design [6].

it is a question to credit the corresponding optimization results. Even though many analytical methods are claimed to have high accuracy, e.g. in [2], developing such a method can be understandably time-consuming.

Second, the computational cost of FEA is considered to be high. This computational cost includes the cost of FEA codes and the corresponding hardware, which should be powerful enough to support the running of FEA codes. The cost of commercial FEA codes is normally charged according to the number of separate calculations; whereas machine designers prefer parallelized optimization and hope to have simultaneous separate calculations as many as possible, so as to reduce the total calculation time. Therefore, the computational cost of using commercial FEA codes for parallelized machine optimization is normally unaffordable for many academic users. On the other hand, there are open-source codes that are free to use. Generally, these codes demand a certain level of knowledge down inside the software (e.g., knowledge about numerical calculation or specified scripting languages, etc.), or have limited capabilities (e.g., no preprocessing or postprocessing interfaces, no adaptive mesh, incapable to handle 3D/multiphysics problem etc.). According to the authors' knowledge, in the field of electrical machine design, there is no single 3D open-source (or free) FEA package that can cover all the three steps of a FEA (preprocessing, solving and postprocessing) for both electromagnetic and thermal problems.

Ironless permanent magnet generators (iPMGs) have been reported for being lightweight [3], [4], which is attractive for offshore wind power application. iPMG is normally designed at large diameter and small aspect ratio. This feature demands the 3D approach for both electromagnetic and thermal designs. The objective of this paper is to present an approach in which open-source 3D FEA tools are used for the multiphysics design and optimization of iPMG. This paper is constructed as follows: section 2 presents the design specialities of iPMGs, the modelling method and calculation results are given in section 3 and 4, section 5 discusses the challenges of using LCR, and section 6 concludes this paper.

2. Design specialities

iPMG is normally adopted into the wind turbine with the so-called *integration design* approach. Under this design philosophy, the generator shares the supporting structures with the other parts of the wind turbine, such as blades, hub, and nacelle [5]. Fig. 1 shows an industrial design example following this concept. This turbine does not have the conventional hub, and the iPMG is supported with spoked structures integrated to blades and main shaft. In such a way, the whole system weight can be significantly reduced.

A notable feature of this iPMG is its large-diameter structure, which contributes to torque production, but also poses challenges. First, the ring-shape iPMG normally has a small aspect ratio (the machine axial length divided by the machine outer diameter), which demands the 3D approach to investigate the magnetic and thermal field. Second, it is through the air gap that the kinetic power is transformed into electricity, therefore, maintaining a reliable air gap is crucial, considering the external force due to strong wind (even gusts) and internal force due to the generator operation. A small air gap requires a stiff supporting structures, whereas a larger and safer air gap demands more consumption of the expensive PM. Third, the spokes and bearings that support the generator should be capable to withstand the generator gravity, operating torque, rotor to rotor normal stress (if there are multiple rotors), and extreme forces caused by faults. Forth, contrary to conventional generators where the active parts (windings, iron, and PM) are enclosed within a frame to prevent harsh external environment or maintain an enclosed cooling system, large-diameter iPMG may be not enclosed to take advantage of the cooling effect of nature air. However, because of the height difference (can be greater than 20 m) from the generator top to its bottom, there may be different local air flow attacking the generator, in addition, the blades rotation makes the local air flow more complex. Therefore, it can be difficult to estimate the winding temperature. Considering the aforementioned points, the design approach should be capable to address these specialities.

3. Modelling method

The authors previously developed a design strategy for the design and optimization of iPMGs [7], and the high accuracy was confirmed by the lab tests. To limit the calculation load, only the magnetic field was considered in this design strategy. It was assumed that machine thermal reliability can be guaranteed by the setting of the maximum current density and electric load. However, the settings are based on the design experience of low-power iron-cored PMG. Furthermore, commercial codes were used in this design strategy.

In this research, this design strategy is improved to account for the thermal aspect with 3D thermal FEA, and all the calculation tools are open-source codes. The upgraded design procedure is illustrated in Fig. 2. The calculation starts with the stator sizing, then the flux density in the air gap is calculated in 3D static FEA with the given dimension. Afterwards, the maximum winding temperature at rated load is obtained in 3D thermal FEA. Finally, the value of the fitness function is calculated. This design approach is driven by a genetic algorithm (GA) optimization code, which manages the GA routine including initialisation, producing new population and generation, and the evaluation of the stopping criteria.

In this research, the three steps for a FEA (preprocessing, solving, and postprocessing) are handled by different codes (Fig. 3): Salome 6.6.0 [8] (for creating mesh), Elmer 7.0 [9] (for solving multiphysics problems) and Paraview 3.14.1 [10] (for extracting the calculation results). Python is the main scripting language for pre- and postprocessing, whereas the solving routine is written in an Elmer-specified .sif script. Note that the calculations of magnetic field, inductance, and thermal field demand different geometries, and therefore there is no universal mesh for all cases. Unlike commercial codes that have reliable adaptive mesh feature, the user has to make sure that fine mesh is created while using the open-source code. This can be done by increasing the mesh in the air gap.

The optimization tool is the GA of Octave [11]. The optimization process is written in .m script of the Octave. All the calculations are executed sequentially. The population size is determined by the number of free variables, and the number of generations is determined by the convergence of the fitness function.

4. A design example

This section presents a design example that uses the aforementioned design approach.

4.1. Machine type

The topology of this generator is shown in Fig. 4. It has one stator and two rotors. The two rotors always have opposite poles facing each other, in such a way, the main flux goes across the air gap. The stator is sandwiched between the two rotors. Non-magnetic material is used to hold the stator, which is segmented into several physically separated parts to facilitate the transportation. Heavily twisted Litz wires are used to minimize the eddy current loss.

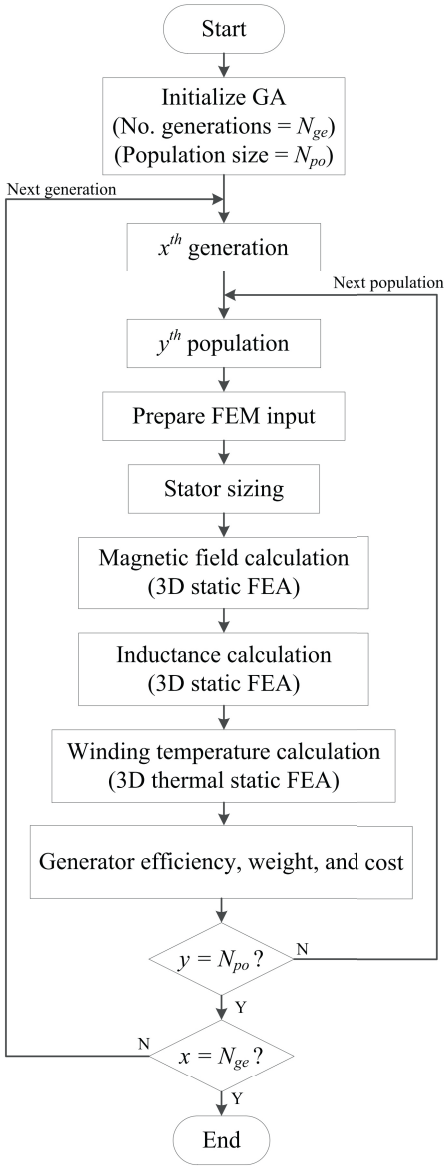

Fig. 2. Design flow chart.

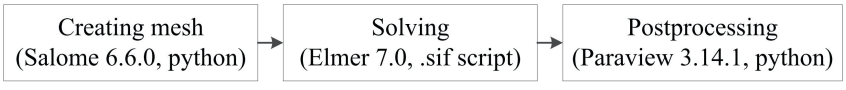

Fig. 3. Flow chart of the 3D FEAs.

4.2. Design specifications and assumptions

The studied machine is a 10 MW iPMG (Table 1). The stator has 9 segments, and coil fill factor is low due to the use of Litz wires. Material prices fluctuate as the market changes. The specific costs provided are based on the authors' industrial experience. Free variables are the inputs for the GA. The valid design outputs should meet the listed constraints. h_M and h_{ry} are used as the free variables instead of B_{p1}, because these two variables are more

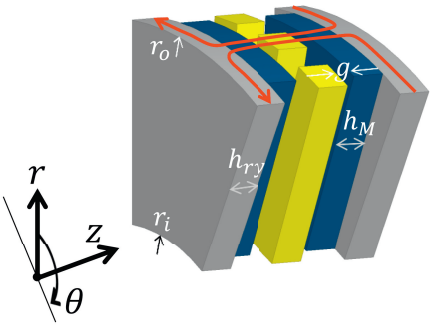

Fig. 4. Machine topology.

straightforward. Selecting σ as the free variable makes the active length directly obtained, in such a way, the back-EMF can be easily calculated for the given dimension after the magnetic field calculation. The thermal reliability is maintained by setting a constraint on the maximum winding temperature rise.

According to IEC standard, for a F-class insulation, the maximum winding temperature rise is 90°C for a 40°C ambient with direct air cooling. The winding thermal conductivity is anisotropic because of the insulation. The radial component of the winding conductivity is close to that of the pure copper; the components of the z and θ axes are dependent on wire type and the detail layout of the coil cross section. In this research, they are assumed to be same, and the equivalent thermal conductivities of these two axes are specified according to [12] (randomly distributed round wires, fill factor is 0.5). In large PM machines, the PM pole normally consists of several small PM blocks. This formation may influence the thermal conductivity along the segmentation direction. In this research, the main cooling path is in the z direction, and the segmentation will not happen in this direction. Therefore, the impact of segmentation is ignored. The rotor yoke is made of solid iron, the thermal property of rotor yoke is therefore isotropic.

4.3. FEA models

To serve the magnetic field analysis, inductance calculation and thermal analysis, different models are used (Fig. 5 - 7).

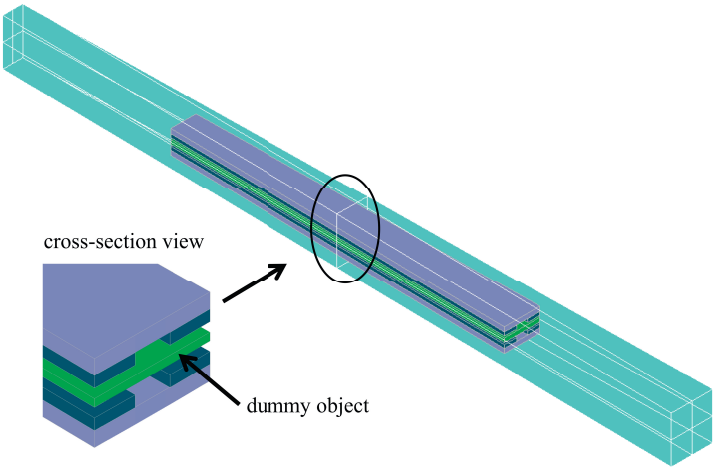

Fig. 5. Field-calculation model.

In the magnetic field analysis, it is of the interest to get the field distribution in the air gap and rotor yoke. To calculate the back-EMF, it is enough to model rotors only. A dummy object is placed between the two rotors for generating a fine mesh in the air gap. Only one pole pitch is modelled to take advantage of the machine symmetry.

Table 1. Generator specification.

Parameters	**Type**	**Value**
Rated power, MW	*Constant*	10
Number of phases (m)	*Constant*	3
Rated speed (n_N), rpm	*Constant*	12
Rated voltage, kV	*Constant*	6.8
Number of stator segments (n_s)	*Constant*	9
Number of parallel branches (a)	*Constant*	1
Coil fill factor (k_f)	*Constant*	0.5
PM(N42SH) B_r at operating temperature, T	*Constant*	1.2
Permeability of PM	*Constant*	1.05
PM specific cost, /kg	*Constant*	80
Iron (solid steel) specific cost, /kg	*Constant*	16
Copper specific cost, /kg	*Constant*	27
Outer diameter (D_o), m	*Constant*	20
Thickness of the air gap (g), mm	*Constant*	$0.15\%D_o$
Winding thermal conductivity (radial direction), W/(mK)	*Constant*	395
Winding thermal conductivity (perpendicular to radial direction), W/(mK)	*Constant*	0.8
PM pole thermal conductivity, W/(mK)	*Constant*	6
Rotor yoke thermal conductivity, W/(mK)	*Constant*	50
Rated frequency (f)	*Free variable*	10-70
Ratio of inner diameter to outer diameter (σ)	*Free variable*	0.5-0.95
Ratio of PM width to pole pitch (k_M)	*Free variable*	0.1-0.8
Current density (J), A/mm^2	*Free variable*	2-5
Thickness of the PM (h_M), mm	*Free variable*	5-100
Thickness of the rotor yoke (h_{ry}), mm	*Free variable*	5-100
Number of turns per coil	*Free variable*	1-10
Max. flux density in air gap (B_{p1}^{ref}), T	*Constraint*	0.8
Max. flux density in rotor yoke (B_{ry}^{ref}), T	*Constraint*	1.7
Max. winding temperature rise (t),°C	*Constraint*	90
Number of population	-	100
Max. number of generation	-	30

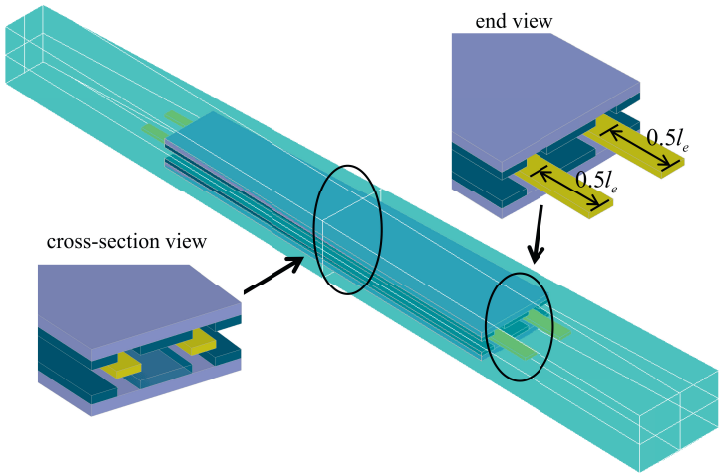

Fig. 6. Inductance-calculation model.

Elmer has special constraints for using the periodic boundary, therefore, it is not a single pole modelled, but two half poles. In such a way, the normal component of the field is set to zero on the symmetry boundaries, which is a boundary type supported in Elmer. The rest four boundaries are in the type of Dirichlet boundary.

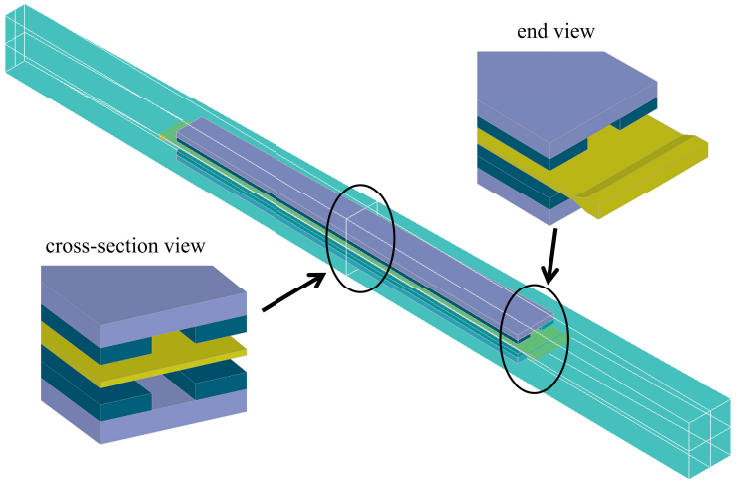

Fig. 7. Thermal model (l_e is the length of single-side end coil).

In the inductance calculation, the method used is to calculate the rated flux linkage, and by dividing this flux linkage with the rated current, the self-inductance will be obtained. In such a process, the magnetization of the PM poles is set to 0, i.e., no saturation in the rotor yoke is taken into account. Because of ignoring the saturation, the calculated inductance will be greater than its real value. Theoretically it is possible to get the inductance by calculating the magnetic energy. However, because Elmer produces much error to get the magnetic energy for a permeability-discontinuous model. Therefore, this method is not used. Two pole pitches are modelled to accommodate one winding, and only the two straight sides of the winding are modelled for simplifying the excitation setting. To take into account the end inductance, the total length of the two straight conductors equals to the total length a complete coil.

The main heat source is the stator copper loss, which is taken away by the convection in the air gap. Accurate accounting for the convection requires the knowledge of the heat transfer coefficient, which is dependent on the machine geometry and local air flow dynamics [13]. CFD analysis is normally required for a good understanding of the air flow. However, this requires the structural design, because the generator for this kind of large structure will normally not have enclosure. The natural air will directly hit the turbine structures including the rotor yoke. Some air will go into the air gap. Meanwhile, the rotor rotation will produce additional air flow, which can help the winding cooling. Therefore, an accurate model should be capable to handle these two air flows. Structural design is out of the scope of this research, air flow and convection are therefore ignored in the thermal analysis. Once the structural design is defined and parametrized, the proposed design strategy can be easily extended to include the CFD analysis. Air gap convection may be replaced with an equivalent thermal conduction [14]. However, this method requires the tests on similar machines for an averaged thermal conductivity. In this research, only heat conduction is considered, and the air equivalent thermal conductivity is set to ten times the thermal conductivity at ambient temperature. The winding is modelled like the practical shape after encapsulation. There is no heat flow in the symmetrical boundaries, and the rest four boundaries are set to ambient temperature.

4.4. Key equations

The iPMG stator is sized according to the approach presented in [7]. There is no need to size the rotor, because the rotor dimension variables are free variables, and the air gap is 0.15% of the outer diameter. With all these inputs, it is ready to do the magnetic field analysis.

The main task of the magnetic field analysis is to calculate the back-EMF. Normally it requires multiple static FEAs or a transient FEA, which can be time-consuming. The method used in this research only employs a single static FEA.

The phase back-EMF (E_{FEA}, in RMS) calculated with FEA is

$$E_{FEA} = \Phi_{p1}\omega_E N_t N_c k_{w1}/\sqrt{2}, \tag{1}$$

where Φ_{p1} is the magnitude of fundamental flux produced by a pole, ω_E is electrical angular velocity, N_t is number of turns per coil, N_c is total number of serially connected coils per phase, k_{w1} is winding coefficient. Φ_{p1} is calculated in the postprocessing of the 3D static FEA.

In the thermal analysis, the main heat source is the copper loss (P_{cu}). This power density for the winding (used at the heat source) is calculated with

$$H_w = \frac{P_{cu}}{m_S} k_f, \tag{2}$$

where m_S is the stator mass. k_f is used to account for the distribution of copper in the stator. Note in practical calculation, the initial copper conductivity is adjusted to that for 90°C. The actual working temperature obtained from the thermal analysis, is used to calculate the copper loss and efficiency. However, to simplified the calculation, this re-calculated copper loss is not used to re-launch the thermal analysis.

3D transient analysis shows that the loss in the permanent magnet is at the level of 1 kW/m^3, therefore, the power density for the permanent magnet is

$$H_M = \frac{1000}{\rho_M} = 0.133 W/kg, \tag{3}$$

where ρ_M is PM density.

The loss in the rotor yoke is very low, thus ignored.

4.5. Calculation result

The objective of this optimization example is to find the optimal design in term of highest efficiency. It took around a week to complete the calculation. The calculation results are given in Table 2. The current density is close to its lower boundary (2 A/mm^2) and k_M is close to the upper boundary (0.8), which are the necessary inputs for achieving high efficiency solution. Air gap flux density is low due to the large equivalent air gap. Note the main component of the air gap field is its component at z axis (Fig. 8). At the ambient temperature (25 °C), the static winding temperature rise is close to the maximum allowable temperature rise. The temperature distribution for the machine end part is given in Fig. 9. Power factor is high due to the ironless structure. For this optimal design, the torque density and power cost are 105.8 Nm/kg and 0.329 euro/W respectively. The calculated efficiency is higher than that given in [7], this may be due to the air gap conduction that underestimates the air cooling. It is possible to get better results by extending the calculation time, however, this was not tried because the purpose is to demonstrate the feasibility of this design strategy.

Table 2. Optimal machine in term of highest efficiency.

Parameters	**Value**
Rated frequency (f)	43.2
Ratio of inner diameter to outer diameter (σ)	0.696
Ratio of PM width to pole pitch (k_M)	0.795
Current density (J), A/mm^2	2.25
Thickness of the PM (h_M), mm	20.25
Thickness of the rotor yoke (h_{ry}), mm	19.15
Number of turns per coil	4
Fundamental flux density in air gap (B_{p1}), T	0.442
Winding temperature rise (t),°C	88.64
Power factor ($cos\theta$)	0.997
Active weight, ton	75.2
Active cost, euro	3.29
Efficiency, %	98.1
Total calculation time, hours	156.32

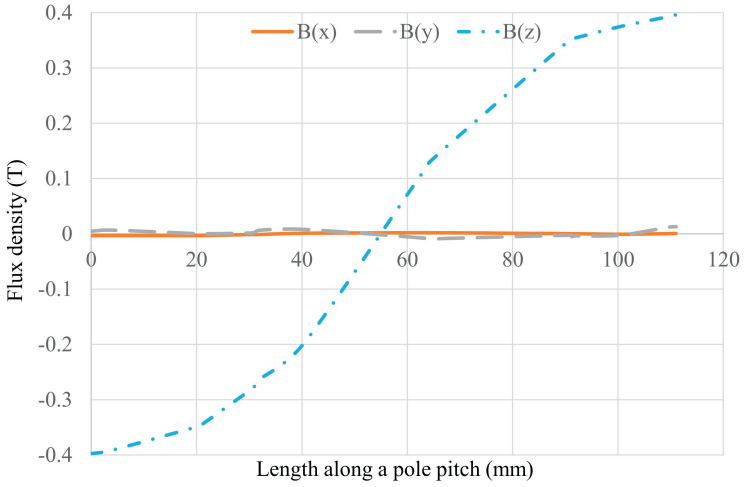

Fig. 8. No-load air gap flux density.

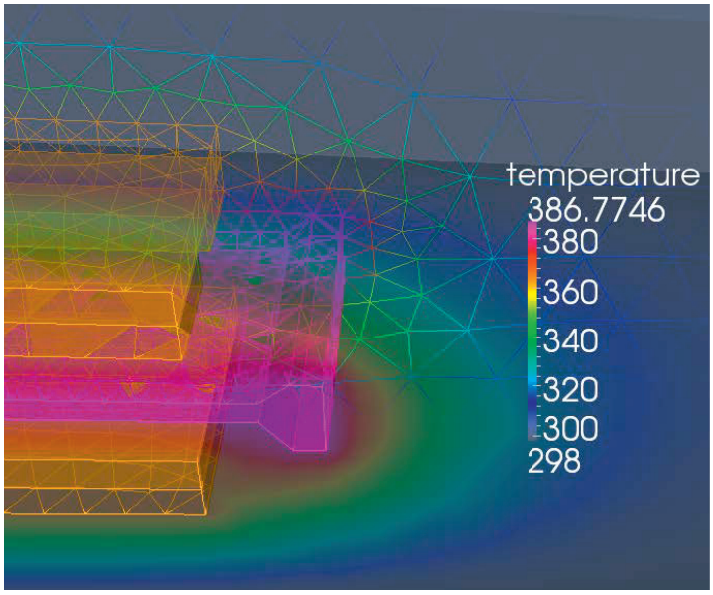

Fig. 9. Machine end part mesh and temperature.

5. Large-scale computing resources

The trick of gaining speedup with LCR is at parallelizing the repetitive calculations. There are two parallel-computing cases. The first one is to ”split” one big calculation into small calculations, e.g., use domain decomposition method to divide a large mesh into several small meshes. Unfortunately, because of the so-called memory wall problem [15], the speedup ratio, depending on many factors (models, algorithm, hardware etc), is normally limited. The commercial code MagNet demonstrates a speedup of approximate 2 from one core to 4 cores [16]. The author’s test shows that there is normally no obvious speedup with the latest commercial FEA codes if the CPU core number is greater than 16, and the maximum speedup is around 5-6. As reported in [17], specific-purpose in-house codes may have better performance, however, so far it is still the game of people focusing on numerical calculation. The second way is to distribute a large amount of independent small calculations over the available computing nodes.

Because of the independence, the speedup ratio can be near linearly increased. This normally fits the need of machine optimization. However, as aforementioned, the computational cost can be very high, because of the need of large number of licenses if commercial codes are used.

Using open-source codes for machine optimization on LCR is attractive, but some problems should be addressed in the design strategy. As a basic requirement, all FEA tools should be parallelized, i.e., no data messed or codes crash, if more than one session are executed simultaneously.

Furthermore, the optimization algorithm should be capable to work together with the job scheduler, so that it is possible to take advantage of the parallelization. Unfortunately, unlike commercial codes that have well-established interface to integrate parallization into optimization algorithms, such open-source codes are still under development. Using message passing interface or similar commands can be an indirect solution, but it demands the scripting skill to piece together the optimization algorithm and parallel mechanism, and depending on the specific parallization method, the optimization performance may be downgraded.

6. Conclusion

To take advantage of LCR for electrical machine design, the corresponding design and optimization strategy has to be studied. A 3D multiphysics design strategy is proposed and investigated in this paper. Open source codes are used for FEA and optimization. A design example is given to show the feasibility of this design strategy. This design strategy enables the possibility of using super computer for machine optimization.

Acknowledgements

This project is supported by Norwegian Research Centre of Offshore Wind Technology (NOWITECH), Norway, and The Petroleum Institute, Abu Dhabi, UAE.

References

[1] Dorrell DG, Ngu SS, Cossar C. Comparison of high pole number ultra-low speed generator designs using slotted and air-gap windings. IEEE Trans. Magn. 2012; vol. 48, no. 11, p. 3120-3123.
[2] Tiegna H, Bellara A, Amara Y, Barakat G. Analytical modeling of the open-circuit magnetic field in axial flux permanent-magnet machines with semi-closed slots. IEEE Trans. Magn. 2012; vol. 48, no. 3, p. 1212-1226.
[3] Spooner E, Gordon P, Bumby JR, French CD. Lightweight ironless-stator PM generators for direct-drive wind turbines. Proc. Inst. Electr. Eng. Electr. Power Appl. 2005; vol.152, no.1, p. 17-26.
[4] Mueller MA, Mcdonald AS. A lightweight low-Speed permanent magnet electrical generator for direct-drive wind turbines. Wind Energy 2009; vol. 12, no. 8, p. 768-780.
[5] Zhang Z, Matveev A, Øvrebø S, Nilssen R, Nysveen A. Review of modeling methods in electromagnetic and thermal design of permanent magnet generators for wind turbines. IEEE ICCEP 2011; Italy, June 2011, p. 377-382.
[6] Norsk 10 MW havvindturbin. Available at: `http://lekegrind.tumedia.no/kraft/2012/10/24/norsk-10-mw-havvindturbin`, last access: 22 Dec. 2013.
[7] Zhang Z, Matveev A, Nilssen R, Nysveen A. Ironless permanent magnet generators for offshore wind turbines. IEEE Trans. Ind. Appl.; to be published.
[8] Salome 6.6.0. Available at: `http://www.salome-platform.org/`, last access: 22 Dec. 2013.
[9] Elmer 7.0. Available at: `http://www.csc.fi/english/pages/elmer`, last access: 22 Dec. 2013.
[10] Paraview 3.14.1. Available at: `http://www.paraview.org/`, last access: 22 Dec. 2013.
[11] Genetic optimization code. Available at: `http://octave.sourceforge.net/`, last access: 22 Dec. 2013.
[12] Nakano T, Kawase Y, Yamaguchi T, Nakamura M, Nishikawa N, Uehara H. Thermal model with winding homogenization and FIT discretization for stator slot. IEEE Trans. Magn. 2011; vol. 47, no. 12, p. 4822-4826.
[13] Howey DA. Thermal design of air-cooled axial flux permanent magnet machines. Ph. D. Dissertation, Imperial College London, 2010; p. 31.
[14] Bastos JP, Cabreira MFRR, Sadowski N, Arruda SR, Nau SL. A thermal analysis of induction motors using a weak coupled modeling. IEEE Trans. Magn. 1997; vol. 33, no. 2, p. 1714-1717.
[15] Iwashita T. Recent technologies for fast electromagnetic field analysis. JMAG User Conference 2008; paper No. 11.
[16] MagNet application example. Simulating a claw-pole alternator in an automobile electrical system environment. Avaialbe at: `http://www.infolytica.com/en/applications/ex0127/`, last access: 22 Dec. 2013
[17] Nakano T, Kawase Y, Yamaguchi T, Nakamura M, Nishikawa N, Uehara H. Parallel computing of magnetic field for rotating machines on the earth simulator. IEEE Trans. Magn. 2010; vol. 46, no. 8, p. 3273-3276.